Supporting Information for: Reassessing the Role of the Indo-Pacific in the Ocean's Global Overturning Circulation

Emily R. Newsom[1] and Andrew F. Thompson[1]

[1] Environmental Science and Engineering, California Institute of Technology, Pasadena, CA, USA

Contents of this file

1. Text S1 to S2
2. Figures S1 to S2

Introduction

These supporting materials provide a schematic to accompanies the derivation of the Buoyancy Transport Framework (Section 2 in the text) in Section S1. In Section S2, we extend our discussion of global buoyancy transport (Section 3 in the text) to address the respective roles of heat and freshwater, and their relationship to observations.

S1. Volume and Buoyancy Transport Schematic

The relationships derived in Section 2 are schematically depicted in Figure S1; relevant quantities are numbered for clarity. We briefly reiterate key relationships from Section 2, which will be used to enumerate terms.

A steady-state balance of volume transport components within volume $V(\sigma, y)$, as defined in the text (i.e. Equation 3 at steady state), requires $0 = \Psi(\sigma, y) - \frac{\partial}{\partial\sigma}\int_V \mathcal{D} dV$. Often, the second term is referred to as water-mass transformation [*Walin*, 1982; *Speer and Tziperman*, 1992], term Ω, were, $\Omega(\sigma, y) = -\frac{\partial}{\partial\sigma}\int_V \mathcal{D} dV$. Therefore, in a steady state,

$$0 = \underbrace{\Psi(\sigma, y)}_{1} + \underbrace{\Omega(\sigma, y)}_{2}. \tag{1}$$

This balance is depicted in Figure S1a.

Corresponding author: Emily Newsom, enewsom@caltech.edu

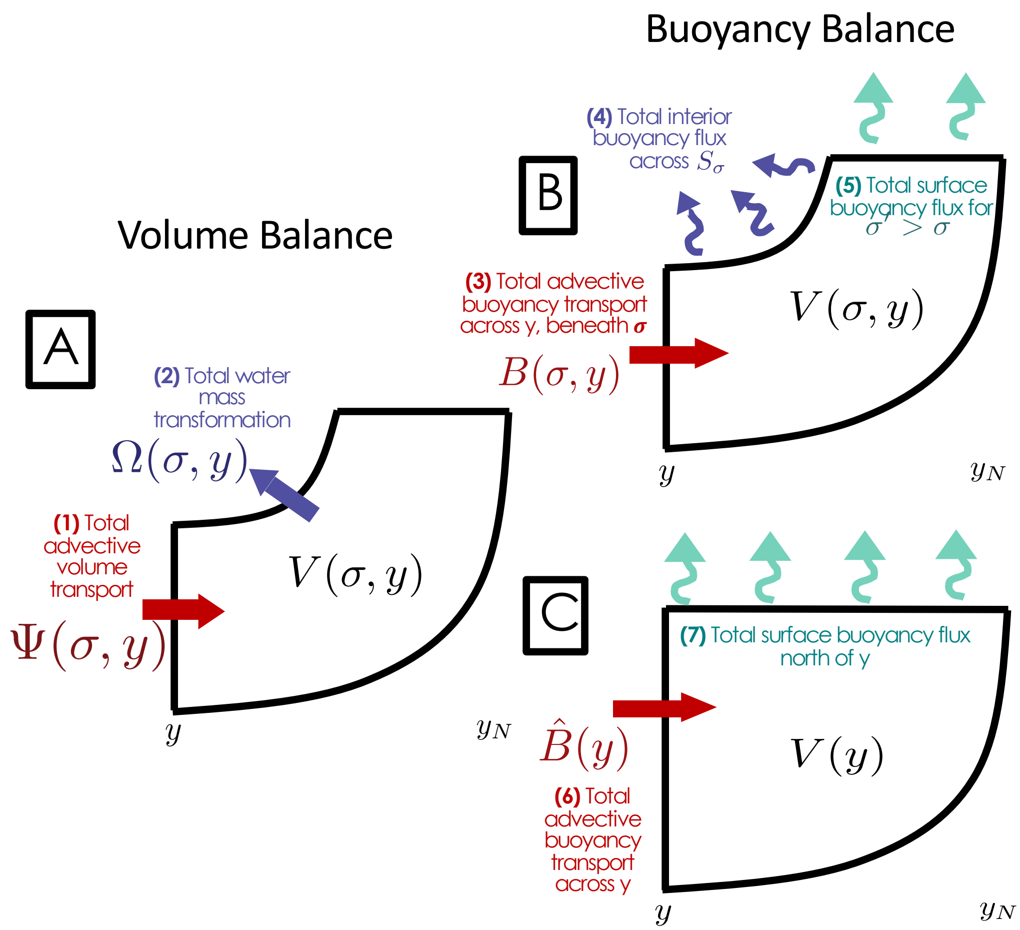

Figure S1. Schematic relationship between components of: A) volume transport into $V(\sigma, y)$, the volume of all waters denser than a given density class, σ, and between latitude y and the northernmost point in the domain, y_N, at steady state; B) buoyancy transport into $V(\sigma, y)$; and C) buoyancy transport in $V(y)$, where $V(y)$ encompasses the full water column at latitude y, and all latitudes to its north. Terms 1-7 are defined in Section S1.

A steady-state balance of buoyancy transport components within $V(\sigma, y)$ requires

$$\underbrace{B(\sigma, y)}_{3} = \underbrace{-\int_{y}^{y_N}\int_{x_E}^{x_W} \lambda_{surf}\mathcal{H}(\sigma_{surf}(x, y) - \sigma)dxdy}_{4} \underbrace{- \int_{S_\sigma} \lambda_{mix}(x, y, z)dS_\sigma}_{5}, \tag{2}$$

where we've combined Eqs. 4 and 5. This balance is depicted in Figure S1b. When $V(\sigma, y)$ is evaluated across the full water column at y, depicted as volume $V(y)$, the only diabatic forcing into $V(y)$ occurs at the surface, such that

$$\underbrace{\hat{B}(y)}_{6} = \underbrace{-\int_{y}^{y_N} \int_{x_E}^{x_W} \lambda_{surf} \, dx dy,}_{7} \tag{3}$$

Eq. 6 in the text. This full-depth case, depicted in Figure S1c, represents the balance between the surface buoyancy flux and the "total residual circulation," $\hat{B}(y) \equiv \frac{g}{\rho_0} \int_{\sigma' > \sigma_{min}(y)} \Psi(\sigma', y) d\sigma'$, where each term is defined in Section 2.

S2. Contributions from Heat and Freshwater

Our study's conclusions center around a dipole in basin-scale surface buoyancy forcing between the Atlantic and Indo-Pacific Oceans in CESM 1.0. This forcing requires southward [northward] buoyancy transport out of the model's Indo-Pacific [into the Atlantic], constraining the GOC structure in each basin, and implicating a zonal exchange of buoyancy facilitated by zonal overturning dynamics south of 30°S. While the intent of the study was to integrate the contributions of heat and freshwater into one tracer, buoyancy, to achieve a direct relationship between surface forcing and GOC structure, here we briefly discuss the respective contributions of heat and freshwater for context.

The large-scale transport patterns central to our conclusions are corroborated by observations. Observationally-based estimates of ocean heat transport vary rather significantly based on methodology [as discussed by *Ganachaud and Wunsch*, 2003], but agree in their estimation of substantial southward heat transport out of the Indo-Pacific and northward into the Atlantic [*Trenberth and Caron*, 2001; *Ganachaud and Wunsch*, 2003; *Large and Yeager*, 2009], sustaining a relatively smaller residual in southward global heat transport across 30°S. In contrast, most observations imply northward freshwater transport into both basins across 30°S [*Ganachaud and Wunsch*, 2003; *Large and Yeager*, 2009], sustaining global net northward freshwater transport across this latitude [*Stammer et al.*, 2004]. *Danabasoglu et al.* [2012] discuss details of the simulation used in our study; they find simulated northward heat transport patterns at 30°S agree well with *Trenberth and Caron* [2001] and *Ganachaud and Wunsch* [2003] and fall within the error bars of *Large and Yeager* [2009]. While *Danabasoglu et al.* [2012] do not address freshwater transport, we note that observed basin-scale differences in heat transport qualitatively support the simulated buoyancy transport patterns we emphasize in our conclusions. Further, observed global southwards [northwards] transport of heat [freshwater] across 30°S corroborate the smaller residual in total buoyancy transport across this latitude found in this study (in Figure 1).

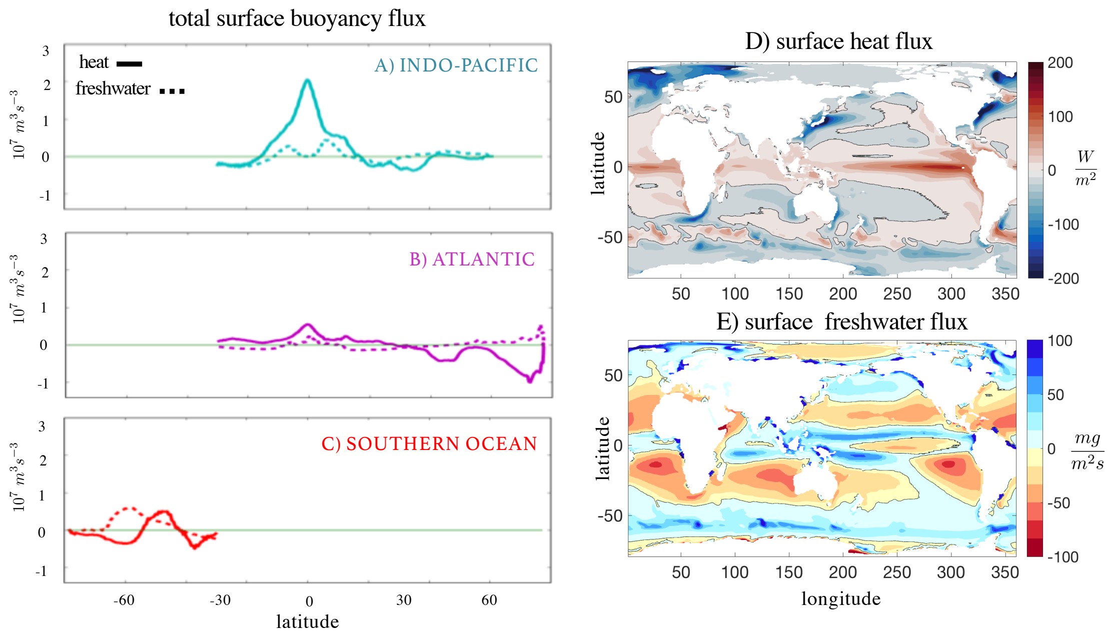

Figure S2. Left column: The respective contributions of heat (solid) and freshwater (dashed) fluxes to the basin-scale total buoyancy flux per latitude (totaled in Figure 1), in the A) Indo-Pacific, B) Atlantic, and C) Southern Ocean. Right column: the spatial distribution of D) heat (top) and E) freshwater fluxes (bottom). Colorscale and units chosen for direct comparison with *Large and Yeager* [2009], Figure 7; *Grist and Josey* [2003] Figures 4 and 7 also provide direct comparisons between observational data sets.

Observational heat and freshwater transport estimates are also broadly consistent with the distribution of surface heat and freshwater fluxes in CESM 1.0. The relative contributions of heat and freshwater (Figure S2) to the total surface buoyancy fluxes (Figure 2a) indicate that heat fluxes contribute primarily to low-latitude buoyancy gain in the Indo-Pacific (Figure S1a) and high-latitude buoyancy loss in the Atlantic (Figure S2b), differences qualitatively supported by observed heat transport patterns, as described above. Freshwater fluxes, while a smaller direct contributor to intra-basin differences in buoyancy forcing, still play a fundamental indirect role in the surface buoyancy flux patterns; the high salinity of warm, northward flowing Atlantic waters predisposes cooling surface waters to sink, sustaining elevated regional heat loss [e.g., *Warren*, 1983; *Weaver et al.*, 1999]. Further, the net freshwater flux in the model's Southern Ocean plays a key role in modifying deep waters upwelled to the surface in that region [*Abernathey et al.*, 2016] and is consistent with observed net northward freshwater transport across 30° S.

While a quantitative assessment of simulated air-sea flux distributions are beyond the scope of the study, the spatial distributions of heat and freshwater fluxes are presented in Figure S2d-e for comparison with observations. Again, observed patterns vary, but the commonalities across observations also agree with the features of simulated patterns emphasized in this study, most obviously high rates of heat flux into in the equatorial Eastern Pacific, and heat loss from the high latitudes of the Atlantic and some regions of the Southern Ocean [*Grist and Josey*, 2003; *Stammer et al.*, 2004; *Large and Yeager*, 2009].

References

Abernathey, R. P., I. Cerovecki, P. R. Holland, E. Newsom, M. Mazloff, and L. D. Talley (2016), *Water-mass transformation by sea ice in the upper branch of the Southern Ocean overturning*, vol. 9, 596–601 pp., doi:10.1038/ngeo2749.

Danabasoglu, G., S. C. Bates, B. P. Briegleb, S. R. Jayne, M. Jochum, W. G. Large, S. Peacock, and S. G. Yeager (2012), The CCSM4 ocean component, *Journal of Climate*, *25*, 1361–1389, doi:10.1175/JCLI-D-11-00091.1.

Ganachaud, A., and C. Wunsch (2003), Large-scale ocean heat and freshwater transports during the world ocean circulation experiment, *Journal of Climate*, *16*(4), 696–705, doi: 10.1175/1520-0442(2003)016<0696:LSOHAF>2.0.CO;2.

Grist, J. P. and S. A. Josey (2003), Inverse Analysis Adjustment of the SOC Air-Sea Flux Climatology Using Ocean Heat Transport Constraints, (Journal of Climate), 3274–3295, doi:10.1175/1520-0442(2003)016<3274:IAAOTS>2.0.CO;2.

Large, W. G., and S. G. Yeager (2009), The global climatology of an interannually varying air-sea flux data set, *Climate Dynamics*, doi:10.1007/s00382-008-0441-3.

Speer, K., and E. Tziperman (1992), Rates of Water Mass Formation in the North Atlantic Ocean, *Journal of Physical Oceanography*, *22*(1), 93–104, doi:10.1175/1520-0485(1992)022<0093:ROWMFI>2.0.CO;2.

Stammer, D., K. Ueyoshi, A. Köhl, W. G. Large, S. A. Josey, and C. Wunsch (2004), Estimating air-sea fluxes of heat, freshwater, and momentum through global ocean data assimilation, *Journal of Geophysical Research C: Oceans*, doi:10.1029/2003JC002082.

Trenberth, K. E., and J. M. Caron (2001), Estimates of Meridional Atmosphere and Ocean Heat Transports, *Journal of Climate*, *14*(16), 3433–3443, doi:10.1175/1520-0442(2001)014<3433:EOMAAO>2.0.CO;2.

Walin, B. G. (1982), On the relation between sea-surface heat flow and thermal circulation in the ocean, *Tellus*, *32*, 187–195.

Warren, B. A. (1983), Why is no deep water formed in the North Pacific ?, pp. 327–347.

Weaver, a. J., C. M. Bitz, a. F. Fanning, and M. M. Holland (1999), Thermohaline Circulation: High-Latitude Phenomena and the Difference Between the Pacific and Atlantic, *Annual Review of Earth and Planetary Sciences*, *27*(1), 231–285, doi: 10.1146/annurev.earth.27.1.231.